Controlled Chainlike Agglomeration of Charged Gold Nanoparticles via a Deliberate Interaction Balance

Hao Zhang,[†,‡] Kin-Hung Fung,[§] Jürgen Hartmann,[†] C. T. Chan,[§] and Dayang Wang*[,†]

Max Planck Institute of Colloids and Interfaces, 14424 Potsdam, Germany, State Key Laboratory of Supramolecular Structure and Materials, College of Chemistry, Jilin University, 130012, Changchun, People's Rebuplic of China, and Department of Physics, Hong Kong University of Science and Technology, Hong Kong SAR, People's Rebuplic of China

Chain-like agglomeration (one-dimensional self-assembly) of aqueous gold nanoparticles (NPs) has been experimentally and theoretically studied. It is demonstrated that the chain growth of aqueous gold NPs is mainly triggered by the anisotropic dipolar interaction due to the Au−S bonding originating from the thiol-ligand capping, plus van der Waals interaction. This anisotropic self-assembly can be endorsed by the isotropic electrostatic repulsion between the gold NPs, which can be finely tuned by the dielectric constant of the surrounding media of the NPs that is dependent on the volume ratio of water to a polar organic solvent. Adding more thiol-ligands or NaCl brings a similar effect of increasing the ionic strength of the NP suspensions, thus lowering the electrostatic repulsion between and, at a certain range, accelerating chain-like agglomeration of the NPs. The use of various thiol-ligands with different terminal groups allow involvement of other interactions, including hydrophobic interaction and hydrogen bonding, between charged gold NPs, which gives rise to a faster kinetic of chain-like agglomeration.

Introduction

The recent advance in wet chemical synthesis of NPs, for instance, via pyrolysis of organometallic precursors in the presence of ligands with long alkyl chains, leads to an exceedingly narrow distribution of both the particle size and the particle shape.[1] This structural monodispersity allows NPs to self-assemble into three-dimensional (3D), highly ordered, and closely packed arrays, colloidal crystals, with new collective physicochemical properties due to the electron or energy transfer between the NPs.[1a,2] Most recently, the elegant design of capping ligands has given rise to a diversity of binary colloidal crystals of NPs.[3] In order to copy the language of molecular self-assembly to organize NPs, current NP research embarks on a shift from the growth of 3D colloidal crystals to the creation of two-dimensional (2D) and one-dimensional (1D) nanostructures. Despite the structural diversification, lower-dimensional self-assemblies of NPs also show a functional resemblance of their molecular analogies. Similar to the polymer chains, for instance, a noticeable elasticity was indeed observed from the chains made from TiO$_2$ NPs.[4]

The apparent simplicity of self-assembly of NPs actually embodies a complicated thermodynamic balance between various attractive and repulsive interactions exerted on the NPs. At the current status, self-assembly of NPs takes places under an isotropic depletion potential, including isotropic van der Waals interaction and an entropy increase of the NP system. Creating an anisotropic interaction potential should be favorable to reduce the spatial dimensionality of self-assembly of NPs. A simple way to do so is to rely on the anisotropic surface chemistry arising from the truncated geometry of NPs with a clear-cut

spatial separation of different crystalline facets. This anisotropic surface chemistry of NPs, especially endorsed after selective modification of different facets with multifunctional ligands, allows covalent spatial coupling of the NPs into clusters or chains. Mirkin et al. have directed self-assembly of differently sized gold NPs into binary clusters via DNA-base pairing of the complementary oligonucleotides.[5] Stellaci et al. have succeeded in giving gold NPs a nanometer-scale analogue of divalent bonding by domain-selective surface modification and directing self-assembly of the NPs into chains.[6] The covalently directed self-assembly of NPs has recently been largely promoted by the success of synthesis of anisotropic and especially Janus NPs. Murphy et al. have selectively patched the two ends of aqueous gold nanorods with biotin and used strepavidin to end-to-end couple the nanorods into chains via the strong interaction between biotin and strepavidin.[7] Kumacheva et al. have implanted directed self-assembly of aqueous gold nanorods via capping their two ends via hydrophobic polymer chains such as polystyrene.[8] Banin et al. have organized gold-tipped CdSe nanorods into structure-defined clusters by linking the gold tips via avidin−biotin interaction.[9]

Different from molecules whose clear-cut spatial separation of different functional groups (at least well-separated hydrophobicity) endorses an anisotropy of the global interaction potential during self-assembly, NPs usually have numbers of interparticle interactions between each other, which depend less on the chemical nature of the surface capping of NPs. The influence of anisotropic surface chemistry designed on NPs may be either suppressed by the isotropic interparticle interactions, such as van der Waals and hydrophobic interaction, or blurred by the anisotropic interactions such as dipolar interaction. In this scenario, therefore, it is necessitated to enhance our understanding of the different roles of various physical interactions during self-assembly of NPs prior to a sophisticated design of the surface chemistry of NPs.

* Corresponding author. E-mail: dayang.wang@mpikg.mpg.de. Fax: +49 331 5679202.
† Max Planck Institute of Colloids and Interfaces.
‡ Jilin University.
§ Hong Kong University of Science and Technology.

Agglomeration of Charged Gold Nanoparticles

J. Phys. Chem. C, Vol. 112, No. 43, 2008 **16831**

Besides their importance in nanoscience, the nanometer dimension of colloidal NPs allows them to be monitored both spatially and temporally. Thus, they can be employed as models for assessing the thermodynamics of atoms, molecules, nuclei, and other elementary particles.[10] From the viewpoint of colloidal science, self-assembly of NPs can be regarded a process of controlled destabilization and agglomeration. The manipulation of NPs in a controlled manner should enable us to gain in-depth insight into various interactions behind condensed matter. Recently, self-assembly of primary NPs has been increasingly recognized as a powerful but nonclassical crystallization way to create superstructured crystals with single crystalline appearance but composed of regularly aligned NPs interspaced with or without molecular or macromolecular spacers. This is extensively exemplified by biomineralization in nature; host of biominerals are mesocrystals.[11] 1D nanocrystal growth via oriented attachment provides another example of this nonclassical crystallization.[12] Formation of single crystalline supracrystals via NP self-assembly has been recently demonstrated by the groups of Han and Cao.[13,14] How the size and shape of supracrystals as a whole are defined during self-assembly of NPs still remains an open question, which requires a better comprehension about the genesis of various nanostructured materials encountered in nature.

Kotov et al. have experimentally and theoretically explored the origin of the local anisotropy of self-assembly of aqueous CdTe NPs under a balance of van der Waals attraction, hydrophobic attraction, anisotropic polar interaction, and electrostatic repulsion.[15] Mann et al. have microscopically and spectroscopically monitored formation of branched chain networks of citrate-stabilized gold NPs by adding 2-mercaptoethanol in aqueous suspensions and correlated the structures of the self-assemblies of gold NPs with their corresponding plasmon resonance spectra. The anisotropic dipolar interactions, arising from anisotropic distribution of the residual surface charges on gold NPs after partially replacing citrate by 2-mercaptoethanol, were accounted by branched chain-like agglomeration (quasi-2D self-assembly) of the NPs.[16] Most recently, we have demonstrated a non-negligible but less-recognized role of interparticle electrostatic repulsion during chain-like agglomeration (1D self-assembly) of negatively charged gold NPs, which can endorse (rather than inhibit as usually thought) the anisotropic agglomeration triggered by the anisotropic dipolar interaction and control the length of the NP chains.[17] Herein, we expand on that previous study and investigate how to deliberately balance various interparticle interactions embodied during self-assembly of charged gold NPs, including van der Waals attraction, dipolar interactions, hydrophobic attraction, electrostatic repulsion, and hydrogen bonding, to warrantee a chain-like controlled agglomeration.

Experimental Section

Materials. Hydrogen tetracholoaurate (HAuCl$_4$, Au 49%) was purchased from Alfa Aesar. Sodium citrate, thioglycolic acid (TGA, 97+%), 3-mercaptopropionic acid (MPA, 99%), thiolactic acid (TLA, 95%), 2-(dimethylamino)ethanethiol hydrochloride (DMAET, 95%), 1-thioglycerol (TG, 98%), L-cysteine (LCS, 99%), and 2-mercaptoethylamine (MA, 98%) were purchased from Aldrich. Scheme S1, Supporting Information, summaries the molecular structures of all thiol-ligands used. All chemicals were used as received.

Preparation of Gold NPs. Citrate-stabilized gold nanoparticles of 15 nm in diameter were prepared in water according to the Frens' method.[18] Briefly, 5 mL of aqueous solution of HAuCl$_4$ (0.1 wt %) was diluted using 45 mL of water in an Erlenmeyer flask, which was heated to boiling. Into the boiling HAuCl$_4$ solution, 1.25 mL of aqueous solution of sodium citrate (2 wt %) was quickly injected under vigorous stirring (the injection time was about several seconds). The reaction solution was kept boiling until its color became red, and then it cooled down to room temperature. The diameters of the resulting gold NPs were determined by transmission electron microscopy (TEM), obtained with a Zeiss EM 912 Omega microscope at an acceleration voltage of 120 kV.

Chain-Like Agglomeration of Gold NPs. The aqueous suspensions of 15 nm gold NPs were used as-prepared without removal of excess of citrate (3.4×10^{11} particle mL^{-1}). Three milliliters of acetonitrile, a mixture of 0.33 mL water and 2.67 mL acetonitrile, and a mixture of 1 mL water and 2 mL acetonitrile was added into 1 mL of gold NP suspension, respectively, in which the volume ratio of water to acetonitrile was 1:3, 1:2, and 1:1. Into the resulting water/acetonitrile suspensions of gold NPs (4 mL) a tiny amount of TGA aqueous solutions (14 mM) was added to initiate agglomeration of gold NPs; the TGA solution volume was varied from 0 to 200 μL. For comparison, 1 mL of as-prepared gold solution was diluted with 3 mL of water, followed by adding 100 μL of 14 mM TGA solution.

In addition to acetonitrile, other water-miscible organic solvents, *N*,*N*-dimethylformamide (DMF; 3 mL) and acetone (3 mL) were added into the aqueous suspensions of gold NPs (1 mL), respectively; the volume ratio of water-to-solvent was set 1:3. Into these suspensions, 50 μL of 14 mM TGA solution was added. In addition to TGA, other thiol-ligands (50 μL, 14 mM), shown in Scheme S1, were also added into water/acetonitrile suspensions of gold NPs (4 mL) in which the water-to-acetonitrile volume ratio was 1:3.

In order to study the effect of ionic strength on the NP agglomeration, varied amounts of aqueous solution of NaCl (1 M) were added into the water/acetonitrile suspensions of gold NPs in the presence of 0.325 mM TGA; the volume ratio of water/acetonitrile was 1:1.

The original pH of 14 mM TGA solution was 2.7. In another set of trials, the pH of the TGA solution was adjusted in the range of 7.5−10.3 by using 1 M NaOH to explore the effect of ionization of TGA on the agglomeration of gold NPs. In this case, the volume ratio of water to acetonitrile was set as 1:3.

After the mixtures containing gold NPs, thiol-ligands, water, and water-miscible organic solvents stood for a certain time, the evolution of the plasmon resonance band of the gold NPs was monitored by absorption spectroscopy preformed on a Cary 50 UV−vis spectrophotometer. The resulting NP aggregates were visualized by TEM.

Calculation of the Plasmon Absorption Spectra of Gold NP Chains. The optical absorption of gold NP aggregates was calculated by the multiple-scattering theory.[19] We used the experimentally measured dielectric function (ε_{Au}) of gold,[20] plotted in Figure S1A, Supporting Information, for modeling. We considered gold nanoparticles embedded in a medium (aqueous solution) with a dielectric constant $\varepsilon_b = 1.96$ (i.e., refractive index $n = 1.4$). For small isolated metal particles, the dominant electromagnetic resonant mode is the Fröhlich mode.[21] The resonance wavelength can be estimated as the wavelength at which the dielectric function of the gold and the medium satisfy the condition $\varepsilon_{Au} = -2\varepsilon_b$. Since gold absorbs light (i.e., ε_{Au} is a complex number), the Fröhlich condition cannot be satisfied exactly. Though, there exists a strong resonance at the wavelength where Re (ε_{Au}) = $-2\varepsilon_b$, and the

resonance appears as an absorption peak. The absorption cross section for single gold NP with diameter $d = 15$ nm indicates that the resonance condition is satisfied at the wavelength of 520 nm (Figure S1B). Accordingly, the calculated absorption spectrum of single 15 nm gold NP shows an absorption peak centered at 520 nm.

When gold NPs form a chain-like aggregate, the single particle resonances should couple each other. To illustrate the effect, we chose a prototypical TEM image of a chain of gold NPs to study the coupling effect to see how the single particle resonance evolves into a collective excitation. Despite the shape variation, in reality, all gold NPs were assumed spherical for calculation simplicity. According to the method described in our previous report,[22] the absorption spectrum of such a chain was calculated for unpolarized and polarized normal incident light.

Results and Discussion

In previous work,[17] we found that the capping of TGA on gold NPs can induce a stronger dipolar interaction, which triggered 1D self-assembly of the NPs into chains. The anisotropy of the short-range dipolar interactions converted isotropic electrostatic repulsion between negatively charged gold NPs into anisotropic, which guaranteed a dominant chain-like aggregation of the NPs. The anisotropic 1D self-assembly of TGA-capped gold NPs was manipulated via the electrostatic repulsion between the NPs. Of importance was that the dielectric constant of the NP media provided a rather fine measure to control the electrostatic repulsion. The use of the mixtures of water/acetonitrile (to decrease the dielectric constant) led to a better control of the NP chain length. In the present work, we systematically used different water-miscible organic solvents and different thiol-ligands at different concentrations so that almost all interparticle interactions encountered in an aqueous self-assembled system of charged pieces, including van der Waals attraction, dipolar interactions, hydrophobic attraction, electrostatic repulsion, and hydrogen bonding, were introduced and, meanwhile, altered between charged gold NPs. In the following sections of this article, the influence of these interparticle interactions on the chain-like agglomeration of charged gold NPs is treated in detail.

Chain-Like Agglomeration of TGA-Capped Gold NPs in Water/Acetonitrile Mixtures. Aqueous suspensions of 15 nm gold NPs, stabilized by citrate, exhibit a ruby color, corresponding to a plasmon absorption band centered at 520 nm. Mixing 1 mL aqueous suspension of citrate-stabilized gold NPs with 3 mL acetonitrile caused little change of the apparent color and the plasmon absorption profile of the gold NPs within at least days. As soon as 14 mM aqueous solution of TGA was added into the mixture suspensions, the absorption tail of the plasmon absorption band of the gold NPs increased and gradually developed into a pronounced absorption band in the wavelength range of 600−800 nm with the increase of the TGA amount added and/or of the storage time, seen macroscopically as a color change from red to blue (Figure 1A−C). Within 1 min after addition of 25 μL of 14 mM TGA into 4 mL of a water/acetonitrile (1:3) suspension of gold NPs, the mixture suspensions exhibited short gold NP chains, visualized by TEM (Figure 1D). Our calculation suggested that, when 1 μL of TGA aqueous solution was added to 4 mL aqueous suspension of 15 nm Au NPs (3.4×10^{11} particle mL^{-1}), the minimal concentration of TGA required for coating the whole surface of the gold NPs was 0.0035 mM. As a result, once 1 μL of 14 mM TGA aqueous solution was added into the suspension, the gold NPs should
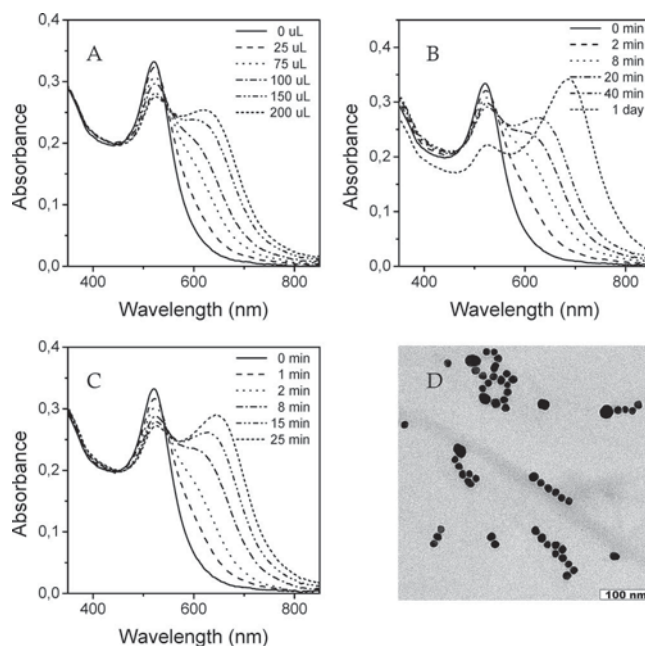

Figure 1. (A) The absorption spectral evolution of a 1:3 (v/v) water/acetonitrile suspension of 15 nm gold NPs versus the amount of 14 mM aqueous solution of TGA added: 0 μL (solid curve), 25 μL (dashed curve), 75 μL (dotted curve), 100 μL (dash-dotted curve), 150 μL (dash-dot-dotted curve), and 200 μL (short-dashed curve). The spectra are recorded 1 min after the TGA addition. The temporal evolution of the absorption spectra of a 1:3 (v/v) water/acetonitrile suspension of 15 nm gold NPs after adding 25 μL (B) and 50 μL (C) of 14 mM aqueous solution of TGA. (D) TEM image of a 1:3 (v/v) water/acetonitrile suspension of 15 nm gold NPs obtained 1 min after adding 25 μL of 14 mM aqueous solution of TGA.

be capped by TGA rather than by citrate. As indicated in Figure 1, TGA plays a pivotal role to trigger 1D self-assembly of gold NPs into chains. Once gold NPs agglomerate into chains, the longitudinal coupling of the plasmon electrons of neighboring NPs along the chains should therefore account for the appearance of the absorption band at the long wavelength range.

Note that the replacement of citrate with TGA on gold NPs also reduced the surface charge density of the NPs due to the difference of the number of carboxylic groups between TGA (one carboxylic group) and citrate (three carboxylic groups), thus lowering electrostatic repulsion between the NPs. As a result, the increase of the TGA amount added promoted chain-like agglomeration of gold NPs (Figure 1A).

When the TGA concentration in the NP suspension was lower than 0.035 M (adding 10 μL of 14 mM TGA into 4 mL of the water/acetonitrile suspension of gold NPs), the resulting blue suspension remained stable for days; little noticeable precipitation of NPs was visible. After the mixture suspensions of gold NPs stood without disturbance for 1 day at the TGA concentration of less than 0.035 M, the further change of both their absorption band maxima and the length of the NP chains, 20−30 NP per chain, inside the suspensions was negligible, which was little dependent on the concentration of TGA (Figure 2).

Calculation of the Plasmon Absorption Spectrum of a Chain Composed of 15 nm Gold NPs. In the current work, the plasmon absorption spectrum of a gold NP chain was calculated on the basis of the multiple-scattering theory that is well-known to be very accurate for calculating the electromagnetic scattering resonance of metallic particles aggregates. The chain geometry was precisely deduced from the TEM image of a prototypical gold NP chain, while all constituent NPs were
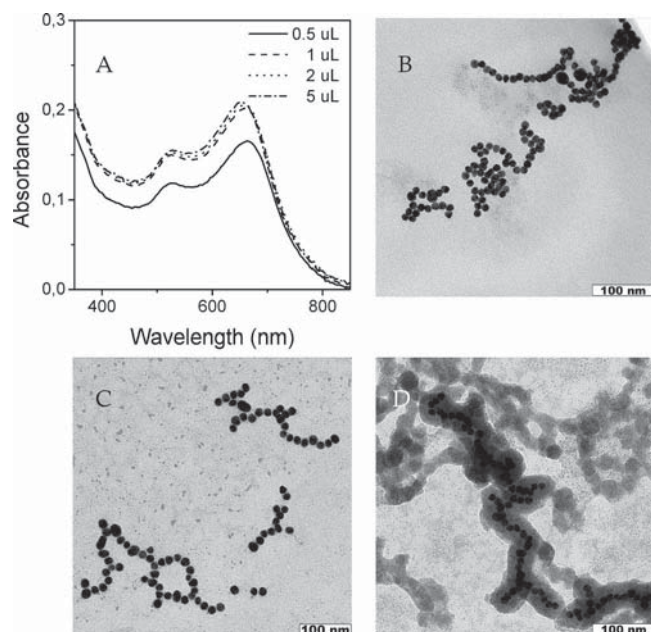
Agglomeration of Charged Gold Nanoparticles

J. Phys. Chem. C, Vol. 112, No. 43, 2008 **16833**

Figure 2. (A) Absorption spectra of a 1:3 (v/v) water/acetonitrile suspension of 15 nm gold NPs obtained after addition of 14 mM TGA aqueous solution: 0.5 μL (solid curve), 1 μL (dashed curve), 2 μL (dotted curve), and 5 μL (dash-dotted curve). TEM images of aliquots of the gold NP suspensions obtained by 0.5 μL (B), 1 μL (C), and 2 μL (D) of 14 mM TGA solutions. The spectra and TEM images were recorded 1 day after TGA addition.
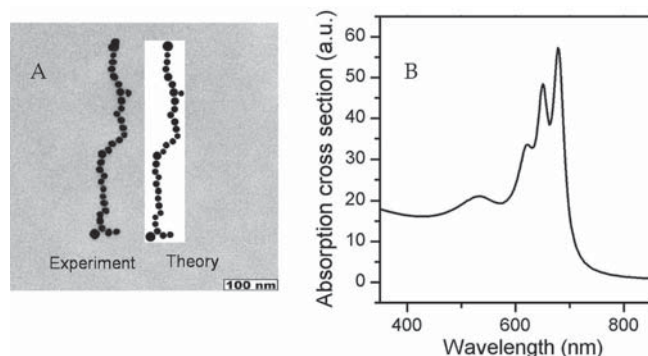
Figure 3. (A) TEM image of a chain comprising 32 gold NPs, indicated as "Experiment". The inset shows the geometrical configuration of the chain, indicated as "Theory". (B) The calculated absorption cross section as a function of wavelength under excitation with unpolarized normal incident light.

assumed spherical in shape for calculation simplicity, as shown in the inset of Figure 3A, and close-packed.[17] We first calculated the absorption spectrum of the NP chain for unpolarized normal incident light. As shown in Figure 3B, an absorption peak centered at 520 nm was visible, that was rather close to the Fröhlich mode resonance of single gold NP of 15 nm size (shown in Figure S1B). This suggests that this absorption peak is dominated by the excitation of the electromagnetic field polarized perpendicular to the NP chain axis.

At the same time, three absorption peaks appeared in the wavelength range from 600−800 nm (Figure 3B). In order to elucidate the origin of these peaks at long wavelength, second, we calculated the absorption spectrum of the NP chain for light polarized parallel to the longitudinal direction of the chain (Figure 4). As shown in Figure 4A, the group of multiple peaks at the wavelength range of 600−800 nm was dominated by the excitation of the electromagnetic field polarized parallel to the NP chain axis. The exact resonance wavelength of these peaks

shifted slightly depending on the geometric characteristics of a particular chain configuration, but all were able to be traced to the longitudinal (along chain axis) plasmon excitations of the chain (Figure 4B−D). In the case of an ensemble of different chains with different geometric configurations, all of these three peaks were calculated to merge into one single broadband.

In order to understand the evolution of the plasmon resonance from individual NPs to NP chains, we artificially decomposed the NP chain shown in Figure 3A into several fragments and repeated the aforementioned calculation procedure, as shown in Figure 5. The calculation indicated that the transverse plasmon resonance of the NP chain at 520 nm remained little changed. In contrast, the longitudinal plasmon resonance in the wavelength range of 600−800 nm blue-shifted, and its band profile was reduced from three peaks to a shoulder peak nearby the transverse plasmon resonance band. In the limit that the chain was broken up into completely isolated NPs (Figure 5G), the longitudinal resonance peak disappeared and the absorption band became the same as that of one single particle (Figure 5H).

As results, the calculated spectra of the chains of gold NPs were consistent with the experimental ones in terms of the plasmon resonance. This manifests that the absorption spectra observed in suspensions of gold NPs should truly represent the collective plasmon resonance of gold NP chains, thus demonstrating that the chains observed on TEM images have been already formed in the suspensions rather than by drying during the TEM sample preparation. On the other hand, the calculated absorption spectra of gold NP chains with different length were in line with the absorption spectral evolution with either the amount of TGA added or the incubation time of TGA in the NP suspension. Thus, the variation of the longitudinal plasmon resonance band observed should be correlated with that of the NP chain length.

The Effect of TGA Ionization. Due to the huge excess of citrate, the aqueous suspension of citrate-capped gold NPs can be regarded as a buffer solution of citrate; its pH is usually around 6.7 after the acidic precursor of $HAuCl_4$ was reduced into gold NPs. Although the pH of 14 mM TGA solution was about 2.7, however, one can infer that addition of TGA into the citrate−buffer suspension of gold NPs gives rise to partial deprotonation of the carboxyl acid terminus of TGA (pK_a 3.53 [24]). As such, the surfaces of the gold NPs should remain negatively charged after the citrate was replaced by TGA. In order to demonstrate this inference, we varied the pH of aqueous TGA solution using NaOH prior to addition into gold NP suspensions. Figure 6 indicates that predeprotonation of TGA can accelerate the chain-like agglomeration of gold NPs, but it is not necessarily needed, which testifies citrate buffering TGA after addition of the TGA into the citrate suspension of the NPs.

The Effect of the Molecular Structures of Thiol-Ligands. In addition to TGA, other thiol-ligands, summarized in Scheme S1, were used to cap gold NPs. According to the terminal group, these thiol-ligands can be classified into three categories: the first terminated with a carboxyl acid group, including TGA, TLA, MPA, and LCS, the second terminated with an amine group, including MA, LCS, and DMAET, and the third terminated with hydroxyl groups, TG. Note that in the citrate buffer suspension of gold NPs (pH = 6.7) the amine terminal group of MA, LCS, and DMAET and the hydroxyl terminal groups of TG remain uncharged, which is different from the carboxylic acid group of TGA, TLA, LCS, and MPA. After these ligands were capped on gold NPs, therefore, interactions other than electrostatic were expected between the NPs, including hydrogen bonding between the amine termini of MA and
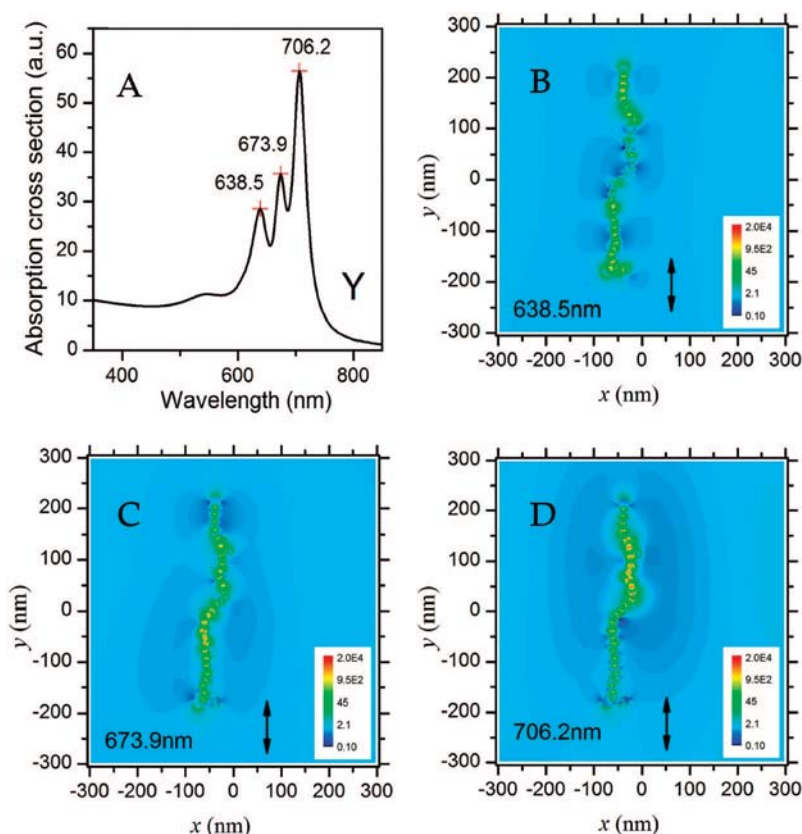
Figure 4. (A) Calculated absorption spectrum of a gold NP chain with the configuration shown in Figure 3A under excitation with light polarized parallel to the longitudinal direction of the chain. The field patterns of the absorption peaks centered at 638.5 nm (B), 673.9 nm (C), and 706.2 nm (D).
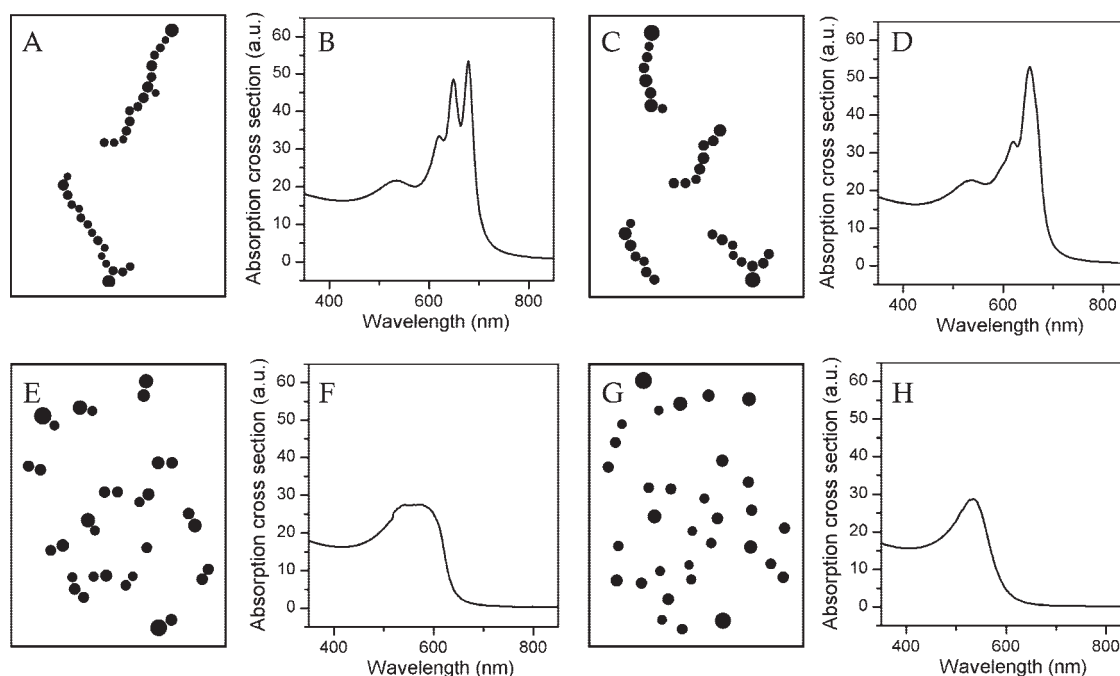

Figure 5. Geometrical configuration of the chains comprising different numbers of gold NPs and their calculated absorption under excitation with light polarized parallel to the longitudinal direction of the chain. Figure parts A and B show the modeling of the chains comprising 16 NPs. Figure parts C and D show the modeling of the chains comprising 8−9 NPs. Figure parts E and F show the modeling of the chains comprising 2−3 NPs. Figure parts G and H show the modeling of single isolated NPs.

the amino acid termini of LCS. In the case of using DMAET to cap gold NPs, the hydrophobicity of the dimethyl amine terminus of DMAET should create the hydrophobic interaction between the capped NPs.[15b]

When TG was used to replace the citrate capping to enhance the dipole moment of gold NPs, the resulting TG-capped NPs remained less agglomerated; only a slight development of the absorption tails was noticed (Figure 7A). This should be due to
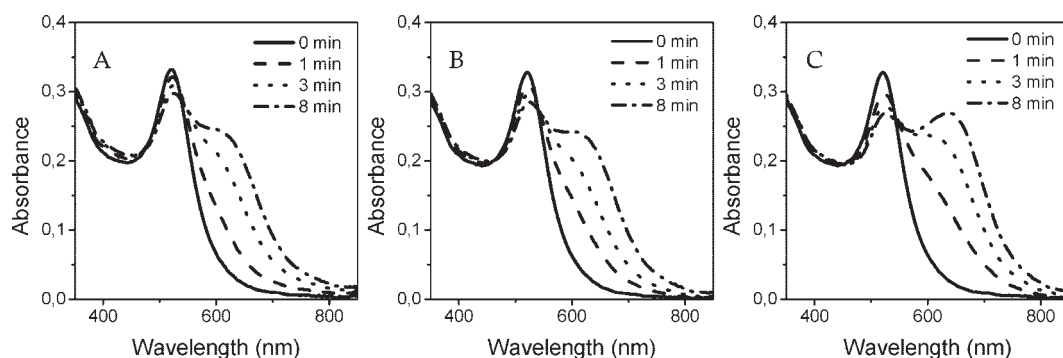
Agglomeration of Charged Gold Nanoparticles

J. Phys. Chem. C, Vol. 112, No. 43, 2008 **16835**

Figure 6. Temporal evolution of the absorption spectra of 1:3 (v/v) water/acetonitrile suspensions of 15 nm gold NPs after addition of 50 uL of 14 mM TGA aqueous solutions: 0 min (solid curve), 1 min (dashed curve), 3 min (dotted curve), and 8 min (dash-dotted curve). Prior to addition, the pH of TGA solution was adjusted to 2.7 (A), 7.5 (B), and 10.3 (C) by using 1 M aqueous NaOH solutions.
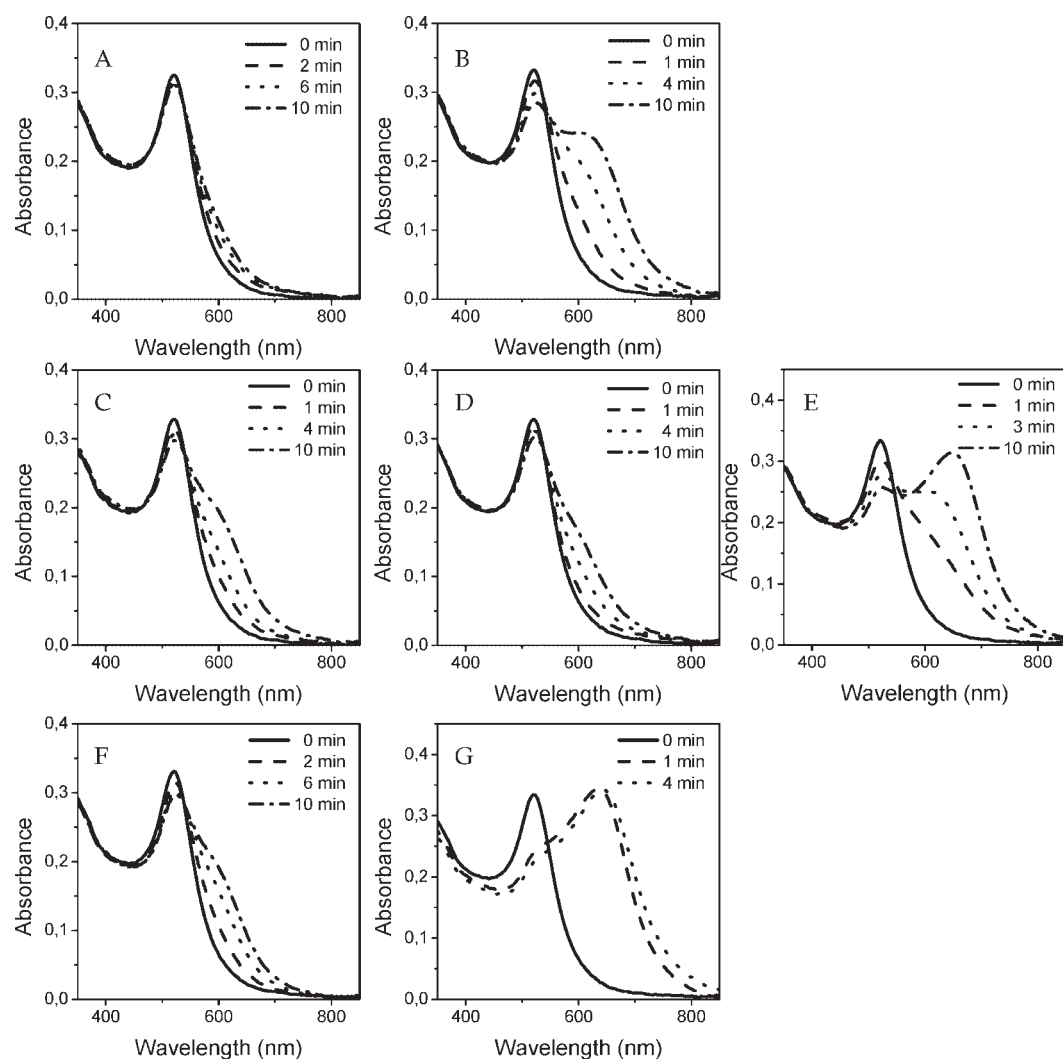

Figure 7. Temporal evolution of the absorption spectra of 1:3 (v/v) water/acetonitrile suspensions of 15 nm gold NPs after addition of 50 μL of 14 mM aqueous solutions of TG (A), TGA (B), TLA (C), MPA (D), LCS (E), MA (F), and DMAET (G) aqueous solutions. After addition of TG or MA, the spectra were obtained after 0 min (solid curve), 2 min (dashed curve), 6 min (dotted curve), and 10 min (dash-dotted curve; figure parts A and F). After addition of TGA, TLA, or MPA, the spectra were obtained after 0 min (solid curve), 1 min, (dashed curve), 4 min (dotted curve), and 10 min (dash-dotted curve; figure parts B–D). After addition of LCS, the spectra were obtained after 0 min (solid curve), 1 min (dashed curve), 3 min (dotted curve), and 10 min (dash-dotted curve; figure part E). After addition of DMAET, the spectra were obtained after 0 min (solid curve), 1 min (dashed curve), and 4 min (dotted curve; figure part G).

the fact that the hydroxyl terminal groups of TG rendered the NPs a better stability against reduction of the electrostatic interparticle repulsion. Similar to TGA (Figure 7B), the other two thiol-ligands, TLA and MPA, caused a noticeable agglomeration after they were added into 1:3 (v/v) water/ acetonitrile suspensions of gold NPs in the presence of huge excess of citrate (Figure 7C,D). After a given time of incubation of the thiol-ligands with gold NPs, TLA and MPA led to a smaller NP agglomeration as compared with TGA, which should be due to the pK_a difference of the carboxyl acid termini of these ligands (the pK_a of TLA and MPA is 3.55 and 4.32, respectively[24]).
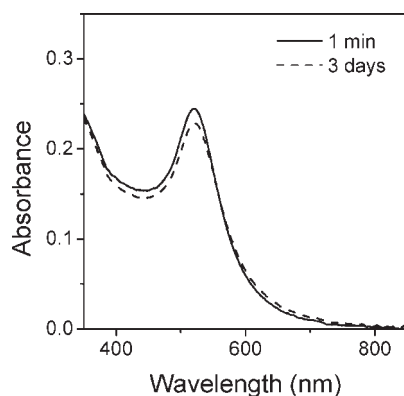
Figure 8. Absorption spectra of an aqueous suspension of 15 nm gold NPs obtained after storage for 1 min (solid curve) and 3 days (dashed curve) after addition of 100 μL of 14 mM TGA aqueous solution. Prior to addition of TGA, 1 mL of as-prepared aqueous suspension of the NPs was diluted into 4 mL.

Figure 7E shows a spectral evolution of the plasmon resonance band of gold NPs in response to LCS. A pronounced absorption band appeared in the wavelength range of 600–800 nm in 10 min after LCS was added, which should be due to the fact that the hydrogen bonding of the amino acid terminal groups of the LCS capping of gold NPs should enhance the attractive interparticle force, thus accelerating the NP agglomeration.

Similar to that of TG, the capping of MA is expected to render the surfaces of gold NPs uncharged, so the MA-capped gold NPs should show a better stability against reduction of electrostatic repulsion between the NPs. Although the hydrogen bonding between the amine terminal groups of the MA capping of neighboring gold NPs should be expected, as shown in Figure 7F, the addition of MA led to a slight aggregation of gold NPs as compared with the addition of LCS.

As shown in Figure 7G, the DMAET capping led to a fast kinetics of chain-like agglomeration of gold NPs; a pronounced absorption centered at 650 nm was observed within 10 min after addition of DMAET to water/acetonitrile (1:3 v/v) suspensions of gold NPs. This fast agglomeration should be due to the hydrophobic attraction of the dimethylamino terminal groups of the DMAET capping of neighboring gold NPs.

The Effect of the Volume Ratio of Water to Acetonitrile. In a control experiment, we diluted 1 mL of as-prepared aqueous suspension of gold NPs into 4 mL with pure water and found that adding as many as 100 μL of 14 mL TGA solution (the TGA concentration was about 0.35 mM) did not cause a change of the plasmon absorption profile of the suspension even after 3 days storage (Figure 8). Note that the TGA concentration gave rise to a noticeable spectral change within 1 min after addition (Figure 1A). This manifests an important role of acetonitrile that should be correlated with the dependence of the electrostatic interaction between identically charged NPs on the dielectric constant of their surrounding media. The relative dielectric constant of acetonitrile (36.6) is smaller than that of water (80.4) at the room temperature. Thus, adding acetonitrile into water should lower the dielectric constant of gold NP suspensions. In the current work, we systematically varied the volume ratio of water to acetonitrile in the suspensions of gold NPs and explored its influence on the chain-like agglomeration of the NPs. To suppress the influence of adding aqueous solutions of TGA on the dielectric constant and on the ionic strength of the surrounding media of gold NPs and to avoid the precipitation of gold NPs during long-term storage, we generally added only a tiny volume of 14 mM aqueous solutions of TGA, less than 50 μL.

Figure 2A shows the absorption spectra of 1:3 (v/v) water/acetonitrile suspensions of gold NPs obtained after 1 day storage at ambient after adding 0.5 μL, 1 μL, 2 μL, and 5 μL into the suspensions, respectively. The spectral profile showed negligible difference for the samples with different TGA concentration. The corresponding TEM images revealed chains composed of 20–40 gold NPs (Figure 2B–D). When the ratio of water to acetonitrile in the suspensions of gold NPs was reduced to 1:2, in contrast, the absorption spectral profile of the NPs showed a noticeable dependence on the amount of TGA added (the concentration of TGA in the NP suspensions; (Figure 9A). The more TGA added, the shorter NP chains were formed. As shown in Figure 9B–F, the gold NP chains composed of 20–40 particles, 10–20 particles, 4–5 particles, and 2–3 particles were obtained after 1 day storage after adding 1 μL, 2 μL, 5 μL, 10 μL, and 20 μL, respectively, into the NP suspensions. This inverse correlation of the length of gold NP chains with the amount of TGA aqueous solutions added was seemingly unexpected and contrary to the aforementioned experimental results that adding more TGA causes more significant agglomeration of gold NPs (as shown in Figure 1A).

As we discussed above, the electrostatic repulsion between gold NPs can be lowered by increasing the ionic strength (adding NaCl and even TGA) and/or by decreasing the dielectric constant of the NP suspensions (adding acetonitrile). Taking this into account, we envisioned that the water-to-acetonitrile volume ratio of 1:2 should be the critical ratio to cause agglomeration of gold NPs; gold NPs remained stable above this point whereas they tended to agglomerate below this ratio. According to this hypothesis, adding more aqueous solution of TGA should raised the water-to-acetonitrile ratio above 1:2, thus enhancing the colloidal stability of gold NPs against agglomeration. While the water-to-acetonitrile ratio in gold NP suspensions was comparable to 1:2, the NPs had a strong tendency to chain-like agglomerates after adding TGA. To explain this, we speculate that the addition of more water may charge the surfaces of TGA-capped gold NPs because of ionization, which increasing the electrostatic repulsion.

The hypothesis was demonstrated by further increasing the water-to-acetonitrile volume ratio to 1:1 in the suspensions of gold NPs. In this case, as shown in Figure 10, gold NPs remained well-separated even after addition of 90 μL of 14 mM aqueous solutions of TGA; no noticeable spectral profile change (Figure 10A) and no NP chains were observed (Figure 10B,C). Adding 120 μL of TGA solution caused a slight increase of the absorption tail above 600 nm (Figure 10A) and led to the chains composed of 4–6 gold NPs (Figure 10D).

In addition to acetonitrile, we also used other water-miscible organic solvents such as DMF and acetone to vary the dielectric constant of the suspensions of gold NPs. The relative dielectric constants of DMF and acetone are 38.3 and 20.7. Here, the water-to-organic solvent volume ratio was set as 1:3 in the suspensions of gold NPs. As shown in Figure 11A, after 50 μL of 14 mM aqueous solution of TGA was added into the suspension of gold NPs, the presence of DMF led to a less pronounced absorption band above 600 nm than the presence of acetone or acetonitrile. This spectral profile difference is well-consistent with the apparent color of these solutions, as shown Figure 11B. The TEM imaging also indicates that gold NP chains formed in the water/DMF suspensions are much shorter than those formed in the water/acetone suspensions (Figure 11C,D). This should be due to the fact that the 1:3 (v/v) water/DMF mixture has the larger dielectric constant (52.1) than the 1:3 (v/v) water/acetone mixture (44.0), so the electrostatic
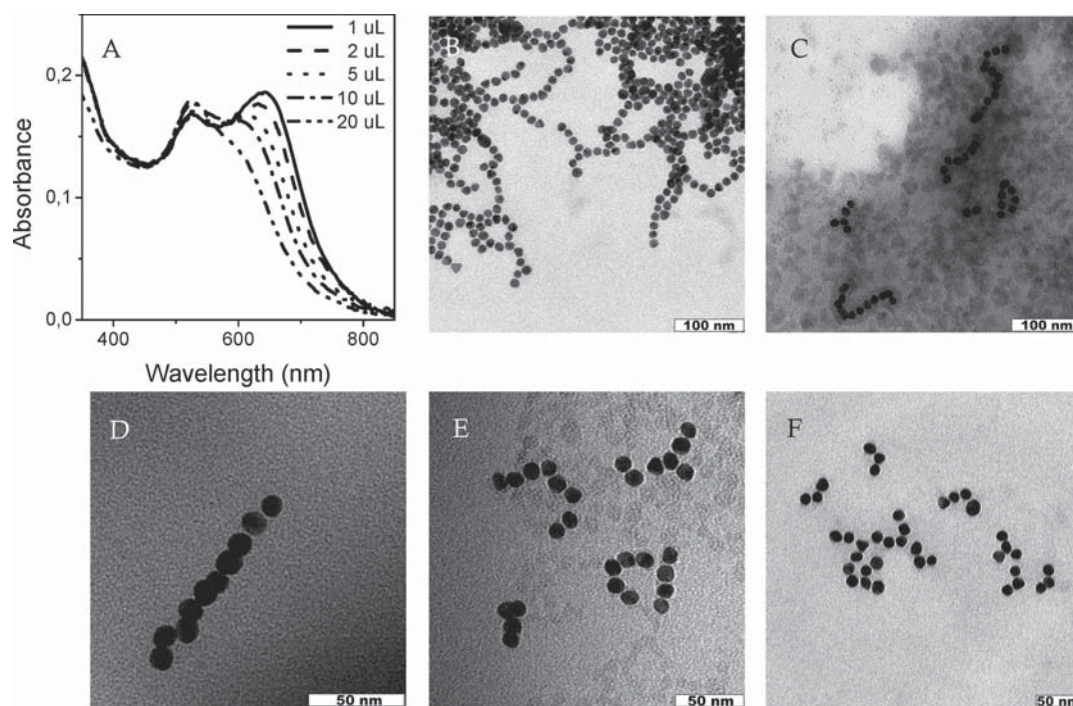
Agglomeration of Charged Gold Nanoparticles

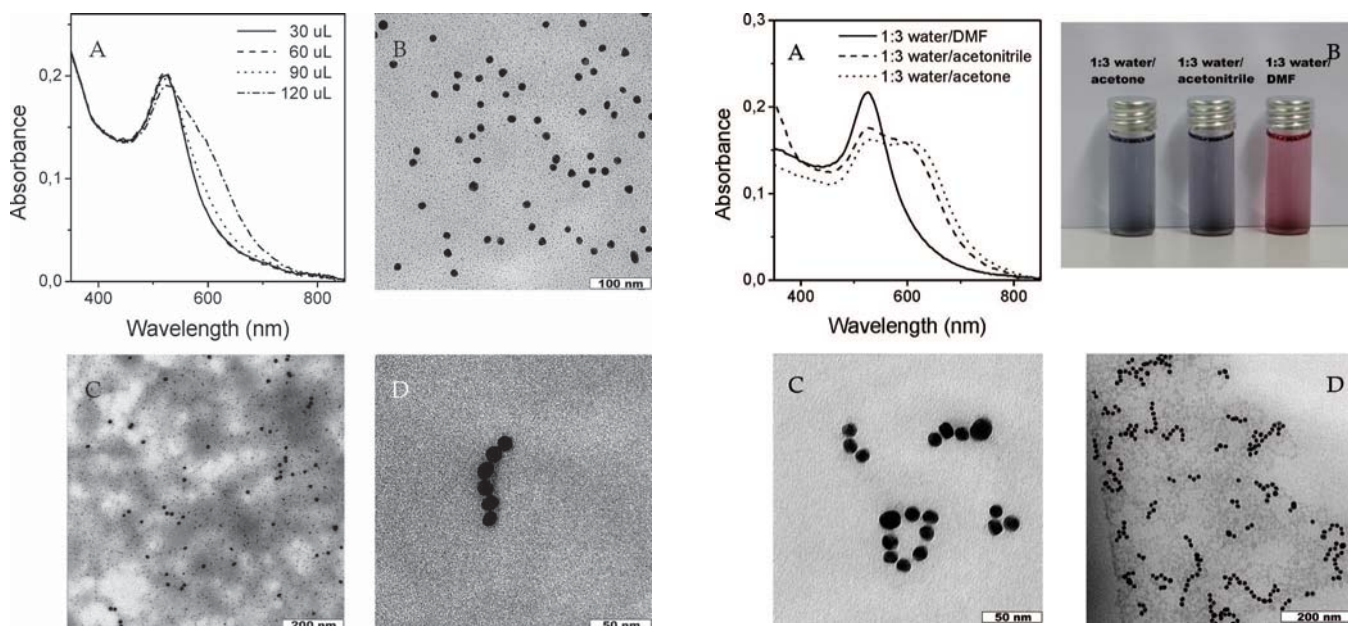*J. Phys. Chem. C, Vol. 112, No. 43, 2008* **16837**

Figure 9. (A) Absorption spectra of a 1:2 (v/v) water/acetonitrile suspension of 15 nm gold NPs obtained after addition of 1 μL (solid curve), 2 μL (dashed curve), 5 μL (dotted curve), 10 μL (dash-dotted curve), and 20 μL (dash-dot-dotted curve) of 14 mM aqueous solution of TGA. (B–F) TEM images of aliquots of the gold NP suspensions obtained by 1 μL (B), 2 μL (C), 5 μL (D), 10 μL (E), and 20 μL (F) of the TGA solutions. The spectra and TEM images were recorded after 1 day storage after TGA addition.

Figure 10. (A) Absorption spectra of a 1:1 (v/v) water/acetonitrile suspension of 15 nm gold NPs obtained after addition of 30 μL (solid curve), 60 μL (dashed curve), 90 μL (dotted curve), and 120 μL (dash-dotted curve) of 14 mM aqueous solution of TGA. (B–D) TEM images of aliquots of the gold NP suspensions obtained by 60 μL (B), 90 μL (C), and 120 μL (D) of the TGA solutions. The spectra and TEM images were recorded after 1 day storage after TGA addition.
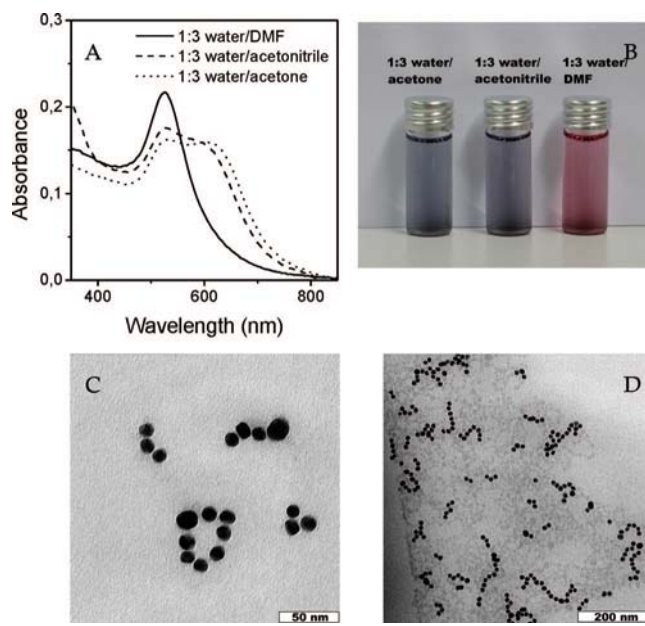

Figure 11. (A) Absorption spectra of a water/DMF (solid curve), water/acetonitrile (dashed curve), or water/acetone (dotted curve) suspension of 15 nm gold NP suspension after addition of 50 mL of 14 mM aqueous solution of TGA. The volume ratio of water to organic solvent is 1:3. (B) Optical photographs of the corresponding suspensions obtained after TGA addition. (C,D) TEM images of aliquots of the water/DMF (C) and water/acetone (D) suspension of the gold NPs. The spectra and TEM images were recorded after 1 h storage after TGA addition.

repulsion between gold NPs in the former was stronger than that in the latter. The optical photographs of the suspensions of the resulting gold NP chains also demonstrate a better colloidal stability of the NP chains during long-term storage (Figure 11B).

The Effect of Ionic Strength. In the previous report, we found that adding NaCl caused chain-like agglomeration of gold NPs in water once the NPs were capped by TGA because of

lowering of the interparticle electrostatic repulsion, which, however, was rather hard to manipulate and to reproduce as compared with the 1D agglomeration triggered by addition of acetonitrile. Here, we studied the salt effect on chain-like agglomeration of gold NPs in a mixture of water and acetonitrile, and the volume ratio of water to acetonitrile was set as 1:1,
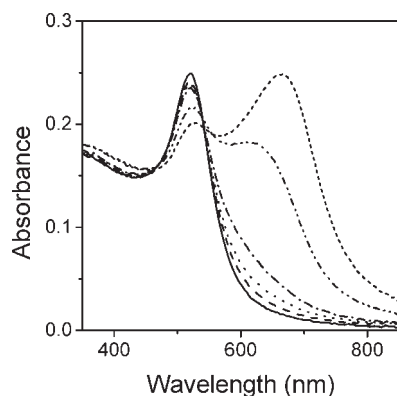
Figure 12. Absorption spectra of 1:1 (v/v) water/acetonitrile suspensions of 15 nm gold NPs obtained after addition of both 14 mM TGA aqueous solution and 1 M NaCl aqueous solutions. The solid curve is the absorption spectrum of the 1:1 (v/v) water/acetonitrile suspension of the gold NPs in the absence of TGA and NaCl. The volume of the TGA solution added is 1 μL. The volume of the NaCl solution added varied from 0 μL (dashed curve), 5 μL (dotted curve), 10 μL (dash-dotted curve), 15 μL (dash-dot-dotted curve), to 20 μL (short-dashed curve). The spectra were recorded after 1 min storage after adding TGA and NaCl.

which caused a rather small agglomeration of gold NPs after addition of TGA. Figure 12 shows that addition of NaCl can accelerate the chain growth of gold NPs; the more NaCl is added, the faster the absorption band at the long wavelength appears. This suggests that the ionic strength of the surrounding media of gold NPs affect the colloidal stability of the charged NPs more than the dielectric constant.

The comparison of Figure 12 and Figure 1 indicates that the effect of adding NaCl on the agglomeration of gold NPs is more significant than that of adding TGA. Adding 20 uL of 1 M NaCl into 4 mL of gold NP suspension (the concentration of NaCl was 5 mM) led to much faster chain growth of gold NPs than adding 200 μL of 14 mM TGA (the concentration of TGA was 65 mM). This result suggests that TGA, at least insofar as a tiny amount (less than 200 μL) was added, mainly enhanced the dipole moment of gold NPs and had a rather small contribution to weakening of the electrostatic repulsion between the NPs.

Conclusion

We have experimentally and theoretically explored chain-like agglomeration of aqueous gold NPs. Systematic investigations reveal the chain-like agglomeration of charged gold NPs as a result of a thermodynamic balance between various interparticle attractive and repulsive forces, including van der Waals attraction, hydrophobic attraction, dipolar interaction, hydrogen bonding, and electrostatic repulsion. The anisotropy of the dipolar interaction, mainly originating from the thiol-ligand capping, is essential for chain-like agglomeration of charged gold NPs. This 1D self-assembly of the gold NPs can be well-manipulated by the electrostatic repulsion between the particles. Other interparticle interactions have a small contribution to direct 1D self-assembly of charged gold NPs, but they have a non-negligible influence on the kinetics of the NP chain growth. As compared with the ionic strength, the dielectric constant of the surrounding aqueous media of gold NPs, which can be finely tuned by adding water-miscible organic polar solvents, provides a rather precise measure to alter the electrostatic interparticle repulsions, thus leading to a fine control of the growth of the NP chains, namely, the chain length.

The future bottom-up nanotechnology is determined by our understanding the correlation of different interparticle interactions with stabilization and agglomeration of colloidal NPs. To program the spatial and temporal sequence of various interparticle interactions should establish new unprecedented ways, supraparticle chemistry,[25] to define the structural complexity of hierarchical self-assemblies of NPs and the collective physico-chemical properties thereof. In the scenario, the thermodynamic picture of balancing various interparticle interactions to control agglomeration (self-assembly) of charged gold NPs should pave one step forward to that direction. In aqueous self-assembled systems, the present anisotropic character of electrostatic repulsion should be taken into account in order to gain in-depth insight into the formation of nanostructures derived from charged nanometer-scale and even subnanometer-scale particles such as nuclei.

Supporting Information Available: Summary of the molecular structures of the thiol-ligands used. Dielectric function of gold and absorption spectrum of single gold NP with a diameter of 15 nm. This material is available free of charge via the Internet at http://pubs.acs.org.

References and Notes

(1) (a) Murray, C.; Kagan, C.; Bawendi, M. *Annu. Rev. Mater. Sci.* **2000**, *30*, 545. (b) Weller, H. *Phil. Trans. R. Soc. Lond. A,* **2003**, *361*, 229. (c) Yin, Y. D.; Alivisatos, A. P. *Nature* **2005**, *437*, 664.

(2) Collier, C. P.; Vossmeyer, T.; Heath, J. R. *Annu. Rev. Phys. Chem.* **1998**, *49*, 371.

(3) (a) Kiely, C. J.; Brust, M.; Bethell, D.; Schiffrin, D. J. *Nature* **1998**, *396*, 444. (b) Shevchenko, E.; Talapin, D.; Rogach, A.; Kornowski, A.; Haase, M.; Weller, H. *J. Am. Chem. Soc.* **2002**, *124*, 11480. (c) Shevchenko, E. V.; Talapin, D. V.; Kotov, N. A.; O'brien, S.; Murray, C. B. *Nature* **2006**, *439*, 55. (d) Shevchenko, E. V.; Talapin, D. V.; Murray, C. B.; O'brien, S. *J. Am. Chem. Soc.* **2006**, *128*, 3620.

(4) Fridtlander, S. K. J. *Nanoparticle Research* **1999**, *1*, 9.

(5) Mucic, R.; Storhoff, J.; Mirkin, C.; Letsinger, R. *J. Am. Chem. Soc.* **1998**, *120*, 12674.

(6) DeVries, G. A.; Brunnbauer, M.; Hu, Y.; Jackson, A. M.; Long, B.; Neltner, B. T.; Uzun, O.; Wunsch, B. H.; Stellacci, F. *Science* **2007**, *315*, 358.

(7) Caswell, K.; Wilson, J.; Bunz, U.; Murphy, C. *J. Am. Chem. Soc.* **2003**, *125*, 13914.

(8) Nie, Z.; Fava, F.; Kumacheva, E.; Zou, H.; Walker, G.; Rubinstein, M. *Nat. Mater.* **2007**, *6*, 609.

(9) Salnt, A.; Amitay-Sadovsky, E.; Banin, U. *J. Am. Chem. Soc.* **2006**, *128*, 10006.

(10) (a) Chow, M.; Zukoski, C. *J. Colloid Interface Sci.* **1994**, *165*, 97–109. (b) Kim, J. C.; Auh, K. H. *Modelling Simul. Mater. Sci. Eng.* **1999**, *7*, 447. (c) Park, J.; Privman, V.; Matijevic, E. *J. Phys. Chem. B* **2001**, *105*, 11630.

(11) Cölfen, H.; Antonietti, M. *Angew. Chem., Int. Ed.* **2005**, *44*, 5576.

(12) (a) Pacholski, C.; Kornowski, A.; Weller, H. *Angew. Chem., Int. Ed.* **2002**, *41*, 1188. (b) Cho, K.-S.; Talapin, D.; Gaschler, W.; Murray, C. *J. Am. Chem. Soc.* **2005**, *127*, 7140.

(13) Zhang, Z.; Sun, H.; Shao, X.; Li, D.; Yu, H.; Han, M. *Adv. Mater.* **2005**, *17*, 42.

(14) Zhuang, J.; Wu, H.; Yang, Y.; Cao, Y. *Angew. Chem., Int. Ed.* **2008**, *47*, 2208.

(15) (a) Tang, Z.; Kotov, N. A.; Giersig, M. *Science* **2002**, *297*, 237. (b) Tang, Z. Y.; Zhang, Z. L.; Wang, Y.; Glotzer, S. Z.; Kotov, N. A. *Science* **2006**, *314*, 274.

(16) Lin, S.; Li, M.; Dujardin, E.; Girard, C.; Mann, S. *Adv. Mater.* **2005**, *17*, 2553.

(17) Zhang, H.; Wang, D. *Angew. Chem., Int. Ed.* **2008**, *47*, 3984.

(18) Frens, G. *Nature Phys. Sci.* **1973**, *241*, 20.

(19) Xu, Y. L. *Appl. Opt.* **1995**, *34*, 4573.

Agglomeration of Charged Gold Nanoparticles

J. Phys. Chem. C, Vol. 112, No. 43, 2008 **16839**

(20) Palik, E. D. *Handbook of Optical Constants of Solids*; Academic: New York, 1985.

(21) Bohren, C. F.; Huffman, D. R. *Absorption and Scattering of Light by Small Particles*; Wiley: New York, 1983.

(22) Fung, K. H.; Chan, C. T. *Opt. Commun.* **2008**, *281*, 855.

(23) Crespo, P.; Litran, R.; Rojas, T.; Multigner, de la Fuente, M. J.; Sanchez-Lopez, J.; Garcia, M.; Hernando, A.; Penades, S.; Fernandez, A. *Phys. Rev. Lett.* **2004**, *93*, 087204.

(24) (a) Che, T.; Kustin, K. *Inorg. Chem.* **1981**, *20*, 509. (b) Zhang, H.; Zhou, Z.; Yang, B.; Gao, M. *J. Phys. Chem. B* **2003**, *107*, 8.

(25) (a) van Blaaderen, A. *Science* **2003**, *301*, 470. (b) Edwards, E.; Wang, D.; Möhwald, H. *Macromol. Chem. Phys.* **2007**, *208*, 439. (c) Glotzer, S.; Solomon, M. *Nat. Mater.* **2007**, *6*, 557–562.